

Analytical approach to the magneto-fluorescence of triplet excitons

Yan Sun¹ and A.D. Chepelianskii¹

¹*LPS, Université Paris-Saclay, CNRS, UMR 8502, F-91405 Orsay, France*

The fluorescence of triplet excitons and color-centers is strongly dependent on magnetic field that mixes the zero field spin eigenstates that determine the radiative recombination rates back into the singlet ground state through spin-orbit coupling. For films of molecules, and polycrystalline color-centers samples an average over molecular orientations has to be performed to model the magneto-fluorescence lineshapes. This limits our analytical understanding of the lineshapes and complicates the analysis of the fluorescence dependence on magnetic field. Here, we present a framework that allows to average over triplet molecular orientations analytically. Our approach provides very accurate numerical routines computing precisely the averages matrix elements that appear in magneto-fluorescence and semi-analytical approximations that can be used to model experimental traces.

I. INTRODUCTION

Spin dependent fluorescence is central to many quantum sensing techniques that rely on ground-state or excited-triplet spin manifolds [1–3]. The fluorescence yield is governed by the overlap of the spin-wavefunction with the zero-magnetic-field eigenstates that emerge via spin-orbit-mediated intersystem crossing [4–6]. Furthermore, the magnetic-field dependence of the fluorescence lineshape is controlled by the relative orientation between the applied field and the triplet fine-structure axes, which has been seen in diverse systems such as defects in solids like NV centers in diamond [7–9], triplet excitons in organics [10–13] and more recently organic di-radicals [14, 15]. In systems comprising randomly oriented triplets, the observed lineshape thus corresponds to an ensemble average over orientations, which is often computed using Monte Carlo simulations [16–19]. However, relying solely on Monte Carlo averaging makes it difficult to extract analytical insights into the lineshape behavior or to perform a precise theory–experiment comparison, since fitting simulated data to measurements can become time-consuming task.

Here, we introduce an analytical framework for computing the ensemble average of the matrix elements relevant to spin-dependent fluorescence. We develop both a series representation and asymptotic approximations that accurately reproduce the low-field and high-field limits while retaining good accuracy throughout the intermediate magnetic-field regime. For this purpose we introduce a theoretical method to analytically incorporate the effect of magnetic field orientation. The proposed approach reduces computational effort while maintaining fidelity to the physical behavior of triplet excitons. Moreover, it provides a transparent analytic connection between field orientation effects and experimentally observed MPL spectra. The framework presented here offers a new approach for the theoretical treatment of spin-dependent processes in excitonic and molecular systems.

II. THEORY

In the molecular frame the Hamiltonian of a triplet in a magnetic field takes the following form:

$$\hat{H} = D_z \left(\hat{S}_z^2 - \frac{2}{3} \right) + E(\hat{S}_x^2 - \hat{S}_y^2) + \mathbf{B} \cdot \hat{\mathbf{S}} \quad (1)$$

where $\hat{S}_{x,y,z}$ are the spin-matrices for a spin $S = 1$. The eigenvalues of this Hamiltonian are $\lambda_0, \lambda_1, \lambda_2$.

At zero magnetic field eigenvectors are given by $|Z\rangle = |0\rangle$, $|X\rangle = \frac{|1\rangle - |{-1}\rangle}{\sqrt{2}}$ and $|Y\rangle = \frac{|1\rangle + |{-1}\rangle}{\sqrt{2}}$. These states form an orthonormal basis corresponding to spin projections along the Z , X , Y respectively. They obey $\hat{S}_x^2|X\rangle = \hat{S}_y^2|Y\rangle = \hat{S}_z^2|Z\rangle = 0$ and are associated with radiative recombination rates $k_{w,S}^0$ ($w = X, Y, Z$).

Omitting coherence effects in the recombination of superpositions of zero field eigenfunctions, we can write the radiative recombination rate into the singlet ground-state for an eigenstate $|\psi_n(\mathbf{B})\rangle$ at finite \mathbf{B} as:

$$k_n(\mathbf{B}) = \sum_{w=X,Y,Z} k_w^0 |\langle \psi_n(\mathbf{B}) | w \rangle|^2 \quad (2)$$

In this expression the magnetic field dependence of the rates enters only through $|\psi_n(\mathbf{B})\rangle$ [7, 20–22]. The fluorescence yield changes with $k_S(\mathbf{B})$. If the changes of the rates with magnetic field are small, it is possible to linearize the rate equations near their values at $\mathbf{B} = 0$. In this case the isotropic orientation-averaged PL spectrum will be proportional to the angle average of the wave function overlaps $\overline{|\langle \psi_n(\mathbf{B}) | X, Y, Z \rangle|^2}$, where the overbar denotes the isotropic angle averaging. The focus of this work is to compute these averages.

For this calculation it is convenient to make the connection between the wave function overlaps and matrix elements of the fine structure tensor:

$$\Sigma_{z,n} = \overline{\langle \psi_n | \hat{S}_z^2 | \psi_n \rangle} \quad (3)$$

$$\Sigma_{xy,n} = \overline{\langle \psi_n | \hat{S}_x^2 - \hat{S}_y^2 | \psi_n \rangle} \quad (4)$$

The average eigenstate projectors on the zero magnetic field eigenbasis can then be written as:

$$\overline{|\langle \psi_n | Z \rangle|^2} = 1 - \Sigma_{z,n} \quad (5)$$

$$\overline{|\langle \psi_n | X \rangle|^2} = (\Sigma_{z,n} - \Sigma_{xy,n})/2 \quad (6)$$

$$\overline{|\langle \psi_n | Y \rangle|^2} = (\Sigma_{z,n} - \Sigma_{xy,n})/2 \quad (7)$$

The advantage of introducing the quantities Σ is that these values are obtained from derivatives of the eigenvalues λ_n . Thus the powder (isotropic) average of the overlaps $|\langle \psi_n | \mathbf{B} \rangle|^2$ are linked to isotropic averages of the eigenvalues:

$$\Sigma_{z,n} = \frac{2}{3} + \partial_{D_z} \overline{\lambda_n}, \quad \Sigma_{xy,n} = \partial_E \overline{\lambda_n} \quad (8)$$

Since $\text{Tr} \hat{H} = \sum_n \lambda_n = 0$, we have the following identities that connect

$$\sum_n \Sigma_{z,n} = 2, \quad \sum_n \Sigma_{xy,n} = 0 \quad (9)$$

so knowing two of the quantities $\Sigma_{z,n}$ and $\Sigma_{xy,n}$ is sufficient, in the following we will focus on the case $n = 0, 2$.

III. EXPANSION AROUND AVERAGE CHARACTERISTIC POLYNOMIAL

Random matrix theory provides elegant analytical techniques to find analytically the average eigenvalue distribution of eigenvalues [23–25]. However these techniques generally apply to the limit of large matrix dimensions which is not the case here. Computing the average resolvent operator, a central quantity in random matrix theory, is in principle feasible. However even in the simpler case $E = 0$, the resulting expression for the average resolvent becomes very complicated. Moreover even if we find some simplifications, this calculation would give the average distribution of the eigenvalues and not the average of each eigenvalue $\overline{\lambda_n}$, thus an alternative approach tailored for this problem is needed. Here we propose to approximate the averages $\overline{\lambda_n}$ by an expansion around the average characteristic polynomial:

$$\overline{\det(u\hat{I} - \hat{H})} = u^3 - (B^2 + E^2 + D_z^2/3)u + \frac{2}{27}q \quad (10)$$

with

$$q = D_z^3 - 9D_z E^2 \quad (11)$$

Using the Cardan formulas the average characteristic equation has three roots u_0, u_1, u_2 , that can be expressed as function of the discriminant

$$\Delta = (3B^2 + D_z^2 + 3E^2)^3 - (D_z^3 - 9D_z E^2)^2 \quad (12)$$

and through the following expressions (where $\omega = e^{2\pi i/3}$)

$$u_2 = \frac{1}{3} \left[(-q + i\sqrt{\Delta})^{1/3} + (-q - i\sqrt{\Delta})^{1/3} \right] \quad (13)$$

$$u_1 = \frac{1}{3} \left[\omega^2(-q + i\sqrt{\Delta})^{1/3} + \omega(-q - i\sqrt{\Delta})^{1/3} \right] \quad (14)$$

$$u_0 = \frac{1}{3} \left[\omega(-q + i\sqrt{\Delta})^{1/3} + \omega^2(-q - i\sqrt{\Delta})^{1/3} \right] \quad (15)$$

For $D_z > 0$ the eigenvalues u_n are ordered by increasing energy. The subsequent discussion will therefore focus on this regime. The expressions can be $D_z < 0$ obtained by swapping the order of the eigenvalues (ground state eigenvector is given by λ_2 and so forth).

Using the roots of the average characteristic polynomial u_n the eigenvalue equation for an arbitrary \mathbf{B} can be written in the following form:

$$\det(\lambda\hat{I} - \hat{H}) = \prod_{n=0}^2 (\lambda - u_n) - \epsilon \quad (16)$$

where the parameter ϵ characterizes the fluctuations of the characteristic polynomial around its mean value.

$$\epsilon = \frac{D_z(2B_z^2 - B_y^2 - B_x^2)}{3} + E(B_x^2 - B_y^2) \quad (17)$$

clearly for an isotropic average $\bar{\epsilon} = 0$. The random direction of the magnetic field \mathbf{B} only changes the offset of the characteristic polynomial. This occurs because the only term combining λ and powers of B in the characteristic polynomial comes from the Zeeman splitting for which, $\det(\lambda\hat{I} - \mathbf{S} \cdot \mathbf{B}) = \lambda(\lambda^2 - B^2)$. Due to this simple form, it is possible to use the Lagrange inversion theorem to obtain a series expansion in powers of ϵ giving the eigenvalues λ_0 :

$$\lambda_0 = u_0 + \sum_{m=1}^{\infty} \frac{\epsilon^m}{m!} \partial_{z=u_0}^{m-1} \frac{1}{(z - u_1)^m (z - u_2)^m} \quad (18)$$

The advantage of this series over other expansions is that the isotropic averages of the powers $\bar{\epsilon}^m$ can be easily computed. We note that this expansion is valid for any ordering of the eigenvalues λ_n so the expansion for $\bar{\lambda}_1$ can be obtained through the permutation of u_0 and u_1 , and $\bar{\lambda}_2$ through the permutation of u_0 and u_2 . In the following provide only formulas for $\bar{\lambda}_0$ as the formulas for other average eigenvalues can be obtained by simple permutation of the indices.

$$\bar{\lambda}_0 = u_0 + \sum_{m=1}^{\infty} \bar{\epsilon}^m \frac{S_n}{(u_1 - u_0)^{2m-1} (u_2 - u_0)^{2m-1}} \quad (19)$$

The Tab. I provides the expressions for S_n and ϵ^m up to order $m = 4$, we computed these average to order $m = 10$ using the python sympy symbolic calculation packages, and use it to provide efficient python numerical routines implanting the Lagrange summation and its derivatives. The code is available at [26].

n	$\bar{\epsilon}^m$	S_n
1	0	1
2	$\frac{4}{45}B^4(D_z^2 + 3E^2)$	$-3u_0$
3	$\frac{16}{945}B^6D_z(D_z^2 - 9E^2)$	$16u_0^2 - u_1u_2$
4	$\frac{16}{945}B^8(D_z^2 + 3E^2)^2$	$-15u_0(7u_0^2 - u_1u_2)$

TABLE I: Analytical expression for the coefficients of the power series Eq. (19)

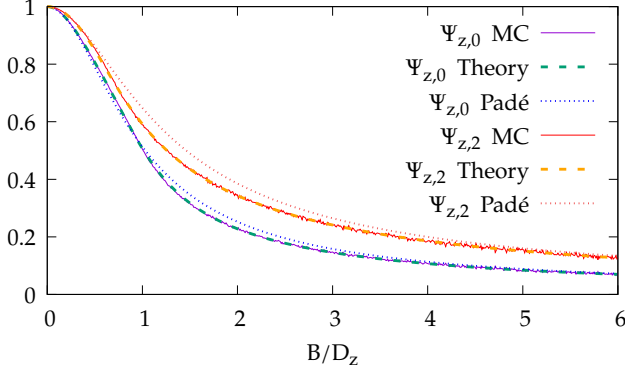


FIG. 1: Isotropic average of $\Psi_{z,0}$ and $\Psi_{z,2}$, the normalized versions of $\Sigma_{z,0}$ and $\Sigma_{z,2}$ defined in Eqs. (20,21), for $E = 0.2D_z$. The averages are computed using a numerical Monte-Carlo method, the series expansion around averaged characteristic polynomial and the semi-analytic Padé approximation (see Tab. II). The difference between MC and the series expansion is within the numerical Monte Carlo noise. The Padé approximation is accurate in the limits $B \rightarrow 0$ and $B \rightarrow \infty$ with sufficient 10% accuracy at $B \sim D_z$, the accuracy is lower in this regime because this approximation takes into account only on the second order term of the power series.

IV. SEMI-ANALYTIC LINESHAPES, COMPARISON WITH MC

To obtain a simpler semi-analytical approximation for the elementary lineshapes $\Sigma_{z,n}, \Sigma_{xy,n}$ we normalize them to look like a positive peak of amplitude 1 at $B = 0$:

$$\Psi_{z,0} = -\frac{3}{2}\Sigma_{z,0} + 1 = \frac{3}{2}\overline{|\langle\psi_0|Z\rangle|^2} - \frac{1}{2} \quad (20)$$

$$\Psi_{z,2} = 3\Sigma_{z,2} - 2 = -3\overline{|\langle\psi_2|Z\rangle|^2} + 1 \quad (21)$$

The averages of $\hat{S}_x^2 - \hat{S}_y^2$, $\Sigma_{xy,2}$ already goes to unity at $B = 0$ and vanishes at $B \rightarrow \infty$ and thus does not need no rescaling.

To describe these lineshapes semi-analytically, we introduce a Padé approximant decomposition:

$$P(B) = \frac{1}{1 + \frac{\alpha_1 B^2}{1 + \frac{\alpha_2 B^2}{1 + \alpha_3 |B|}}} \quad (22)$$

This expression can be viewed as a Lorentzian with B dependent width leading to slower B^{-1} decay at infinity. It has leading even terms B^2, B^4 at $B = 0$ and leading B^{-1} term at $B \rightarrow \infty$. The Padé approximant structure ensures that only even powers of B contribute to the expansion near $B = 0$, the first odd term for Eq. (22) is B^5 , higher order terms in the nested fraction series would give a higher order for the appearance of the first odd power in the expansion around $B = 0$.

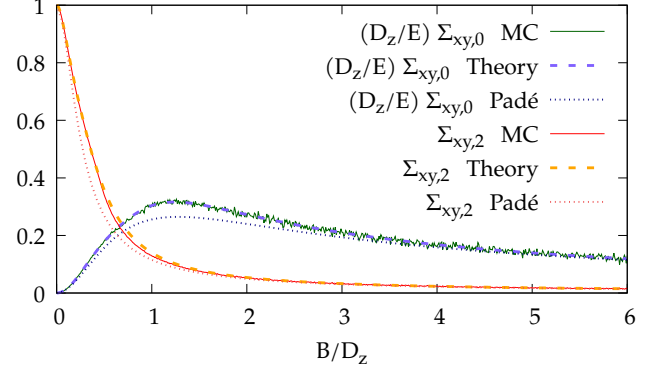


FIG. 2: The isotropic average of $\Sigma_{xy,0}$ and $\Sigma_{xy,2}$ based on the three methods for $E = 0.1D_z$.

The expressions for $\alpha_{1,2,3}$ are then obtained by matching the leading asymptotic terms around $B = 0$ and $B = \infty$ to the power series Eq. (19). Keeping the order ϵ^2 terms gives a simple expression approximation accurate to order B^4 at zero and order B^{-2} at ∞ :

$$\langle \lambda_0 \rangle = u_0 - \frac{4B^4(D_z^2 + 3E^2)u_0}{15(u_2 - u_0)^3(u_1 - u_0)^3} \quad (23)$$

We thus use this expression to fix the values of numerical coefficients $\alpha_{1,2,3}$. The parameters for $\Psi_{z,0}$ and $\Psi_{z,2}$ are essentially fixed by D_z (with E/D_z corrections), while E is the main parameter for $\Psi_{xy,2}$ (with also E/D_z corrections).

Fig. 1 shows the perfect overlap between Monte Carlo averages of $\Psi_{z,n}$ and the summation of the Lagrange inversion series, we used $E = 0.2D_z$ to show that the expression remains accurate even for relatively large values of E . The Padé approximation becomes exact in the limits $B = 0, \infty$, thus the worse error for the Padé approximation is 13% for $\Psi_{z,2}$ at $B/D_z \simeq 1.5$.

The lineshape $\Sigma_{xy,0}$ is zero at $B = 0$ and cannot be approximated by Eq. (22). To approximate it semi-analytically we introduce the linshape:

$$\tilde{P}(B) = \frac{\beta_0 B^2}{(1 + \beta_1 |B|)(1 + \beta_2 B^2)} \quad (24)$$

	α_1	α_2	α_3
$\Psi_{z,0}$	$\frac{1}{D_z^2} + \frac{3E^2}{D_z^4}$	$\frac{0.24}{D_z^2} + \frac{1.6E^2}{D_z^4}$	$\frac{0.6}{D_z} + \frac{2.2E^2}{D_z^3}$
$\Psi_{z,2}$	$\frac{1}{(D_z+E)^2}$	$\frac{4}{5(D_z+E)^2}$	$\frac{1}{D_z}$
$\Sigma_{xy,2}$	$\frac{1}{6E^2} + \frac{1}{D_z^2}$	$\frac{0.28}{E^2} + \frac{-1.23}{D_z^2}$	$\frac{2.1}{E} - \frac{13.5E}{D_z^2}$

TABLE II: Parameters $\alpha_{1,2,3}$ for the Padé approximation Eq. (22) obtained by asymptotic matching of the Lagrange inversion series up to order ϵ^2 (Eq. (23)).

A good approximation to $\frac{D_z}{E} \Psi_{xy,0}$ can be obtained using the values: $\beta_0 = -\frac{4D_z E}{3(D_z^2 - E^2)^2}$, $\beta_1 = \frac{6}{5D_z}$ and $\beta_2 = \frac{25D_z^2}{18(D_z^2 - E^2)^2}$ as shown in Fig. 2.

Fig. 1 also shows the comparison between the Lagrange series and the Monte-Carlo average for $\Sigma_{xy,2}$, we notice that the agreement between Monte-Carlo simulation and Eq. (19) is not perfect and a small discrepancy exists. This is due to the fact that the Lagrange inversion formula is not aware of possible level-crossings between $|\pm 1\rangle$ states and even if the series is convergent it does not necessarily converge to the right root. To account for this we stopped the summation of the Lagrange series at order ϵ^4 for which the best numerical agreement was achieved. The codes for the Lagrange series and Monte Carlo are provided on [26].

These equations Eqs. (22,24) together with Tab. II provide a complete set of semi-analytical approximations for the isotropic average of the matrix elements. The functions $\Psi_{z,n}$ are all very similar even if their precise line-shape differs (see Fig. 1), it will thus be difficult to distinguish their contributions from experimental magneto-photo luminescence traces. The characteristic magnetic field scale is of order D with small corrections of order E^2/D but the numerical prefactors depend on $n = 0, 2$.

For matrix elements of $\Psi_{xy,n}$ the lineshapes for $\Psi_{xy,0}$ and $\Psi_{xy,2}$ are very different. The E term mixes the $|\pm 1\rangle$ states competing with their mixing by the magnetic field, $\Psi_{xy,2}^{xy}$ is thus a narrow peak of the same Padé form as $\Psi_{z,n}$ but with a width mainly fixed by the E value. The mixing of $|0\rangle$ with the two other $|\pm 1\rangle$ states occurs on an energy scale fixed by D but the small anisotropy breaks x, y symmetry perturbatively, the line shape for this matrix element then looks like the field derivative of lineshapes $\Psi_{xy,n}$ with a maximum amplitude of order E/D_z .

Using the relation between the symbols Ψ and matrix elements we find that the lineshape for the matrix overlaps $|\langle \psi_n | Z \rangle|$ ($n = 0, 1, 2$ numbers the triplet eigenstates) is well described by peaks with of order D_z , the semi-analytical parameters are given in Table. 2. For $D_z > 0$, the lineshapes for $|\langle \psi_0 | X, Y \rangle|$ will be a combination of $|\langle \psi_0 | Z \rangle|$ and a derivative looking lineshape. Finally matrix elements $|\langle \psi_{1,2} | X, Y \rangle|$ will be a combination of lineshapes with a width of order D_z and narrower peaks with width E . The case of $D_z < 0$ can be reduced to $D_z > 0$ by flipping the order of the eigenstates

$$n = 0, 1, 2.$$

The calculations were performed for each of the eigenstates separately, which is the case of a strong optical polarization of the spin-states. For a spin-distribution close to thermal equilibrium we may need the thermal averages at temperature T .

$$\Sigma_z = \frac{1}{Z_T} \sum_n e^{-\lambda_n/T} \langle \psi_n | \hat{S}_z^2 | \psi_n \rangle \quad (25)$$

where $Z_T = \sum_n e^{-\lambda_n/T}$ is the normalization. We show numerically that it is justified to neglect correlations in this average, and thus the finite temperature average can be reduced to quantities that we have already computed:

$$\Sigma_z \simeq \frac{1}{Z_T} \sum_n e^{-\lambda_n/T} \Sigma_{z,n} \quad (26)$$

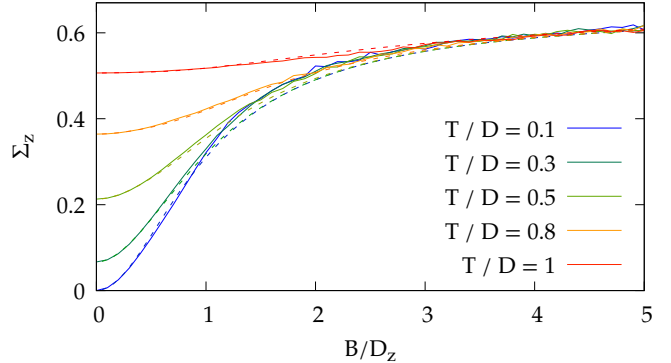


FIG. 3: Monte Carlo simulation of Σ_z the finite temperature averages of the matrix elements for \hat{S}_z^2 introduced in Eq. (25) compared with the uncorrelated approximation Eq. (26). A very good agreement is observed at both low and high temperatures.

The comparison between expressions Eq. (25,26) is shown in Fig. 3, to approximate $\Sigma_{z,n}$ we use Padé approximation Eq. (22) (with Table II) and Eq. (23) for λ_n . We see the uncorrelated approximation gives the finite temperature averages with good accuracy. We notice that in practice the small difference between the Padé approximation and exact lineshapes is likely to be absorbed in a small renormalization of D_z of a few percent. If a systematic high temperature expansion is needed we provide in appendix an identity on the trace of powers of the triplet Hamiltonian that can be useful. It connects the trace of powers of the spin Hamiltonian for $E = 0$ with combinatorics.

V. CONCLUSION

In this work, we proposed a theoretical method to find analytically the average over magnetic field orientation for eigenvalues and matrix elements expected to

appear in the photo-luminescence rate for triplet excitons. We consider the average characteristic polynomial of the spin Hamiltonian and perform an expansion in powers of the orientation-dependent correction terms, allowing to find the analytical order by order averages. We showed the good agreement between analytical series expansion and Monte-Carlo simulations, and derived semi-analytical approximations for the lines-shapes that we expect to appear in experiments. Since the fine-structure parameters D_z and E can be determined from magnetic resonance experiments with high precision, this analytical treatment should allow to link experimental MPL lineshape with spin-dependent recombination rates and triplet state populations.

Acknowledgments

The authors thank R. Chowdhury, R.H. Friend and G. Poly for helpful discussions. This research was supported by funding from ANR-20-CE92-0041 (MARS), and the European Research Council (ERC) under the European Union's Horizon 2020 research and innovation program (grant Ballistop agreement no. 833350).

Appendix A: High temperature expansion

At finite temperature, the average will involve the trace $\text{Tr } e^{-\beta \hat{H}}$

$$\Psi(D_z, B) = \frac{2}{3} - \frac{1}{\beta} \partial_{D_z} \langle \log \text{Tr } e^{-\beta \hat{H}} \rangle \quad (\text{A1})$$

Expansion of the exponential as function of β leads to the trace of successive powers of \hat{H} .

For the trace of powers of $\hat{H} = D_z \hat{S}_z^2 + B_x \hat{S}_x + B_z \hat{S}_z$, we find the following expansion:

$$\text{Tr } \hat{H}^N = \sum_{2n+2m+p=N} T_{n,m,p} B_x^{2n} B_z^{2m} D_z^p \quad (\text{A2})$$

the coefficients are given by:

$$T_{n,m,p} = \frac{(2m+n)N}{(m+n)(N-n)} \binom{n+m}{m} \binom{N-n}{n+2m} \quad (\text{A3})$$

and the sums runs over all integers $n, m, p \geq 0$ obeying the summing condition.

This expression is obtained by noticing that all the traces of the form

$$\text{Tr } \hat{S}_1 \dots \hat{S}_k \quad (\text{A4})$$

where each matrix S_i is either S_x or S_z are all equal to 0 or 1, Eq. (A3) is then obtained by counting the number of non zero configurations [27].

[1] D. D. Awschalom, R. Hanson, J. Wrachtrup, and B. B. Zhou, Quantum technologies with optically interfaced solid-state spins, *Nature Photonics* **12**, 516 (2018).

[2] G. Wolfowicz, F. J. Heremans, C. P. Anderson, S. Kanai, H. Seo, A. Gali, G. Galli, and D. D. Awschalom, Quantum guidelines for solid-state spin defects, *Nature Reviews Materials* **6**, 906 (2021).

[3] M. W. Doherty, N. B. Manson, P. Delaney, F. Jelezko, J. Wrachtrup, and L. C. Hollenberg, The nitrogen-vacancy colour centre in diamond, *Physics Reports* **528**, 1 (2013).

[4] S. L. Bayliss, L. R. Weiss, A. Mitioglu, K. Galkowski, Z. Yang, K. Yunusova, A. Surrent, K. J. Thorley, J. Behrends, R. Bittl, *et al.*, Site-selective measurement of coupled spin pairs in an organic semiconductor, *Proceedings of the National Academy of Sciences* **115**, 5077 (2018).

[5] Y. Sun, M. Monteverde, V. Derkach, T. Chaneilie, E. Aldridge, J. Anthony, and A. Chepelianskii, Spin dependent fluorescence mediated by anti-symmetric exchange in triplet exciton pairs, *arXiv preprint arXiv:2502.07038* (2025).

[6] L. Robledo, H. Bernien, T. Van Der Sar, and R. Hanson, Spin dynamics in the optical cycle of single nitrogen-vacancy centres in diamond, *New Journal of Physics* **13**, 025013 (2011).

[7] J. P. Tetienne, L. Rondin, P. Spinicelli, M. Chipaux, T. Debuisschert, J.-F. Roch, and V. Jacques, Magnetic-field-dependent photodynamics of single nv defects in diamond: an application to qualitative all-optical magnetic imaging, *New Journal of Physics* **14**, 103033 (2012).

[8] J. F. Barry, J. M. Schloss, E. Bauch, M. J. Turner, C. A. Hart, L. M. Pham, and R. L. Walsworth, Sensitivity optimization for nv-diamond magnetometry, *Reviews of Modern Physics* **92**, 015004 (2020).

[9] K. Veys, M. H. Bousquet, D. Jacquemin, and D. Escudero, Modeling the fluorescence quantum yields of aromatic compounds: benchmarking the machinery to compute intersystem crossing rates, *Journal of Chemical Theory and Computation* **19**, 9344 (2023).

[10] M. Oxborrow, J. D. Breeze, and N. M. Alford, Room-temperature solid-state maser, *Nature* **488**, 353 (2012).

[11] S. L. Bayliss, A. D. Chepelianskii, A. Sepe, B. J. Walker, B. Ehrler, M. J. Bruzek, J. E. Anthony, and N. C. Greenham, Geminate and nongeminate recombination of triplet excitons formed by singlet fission, *Physical review letters* **112**, 238701 (2014).

[12] Y. Sun, M. Monteverde, V. Derkach, J. Anthony, and A. Chepelianskii, Cascade of multiexciton states generated by singlet fission, *The Journal of Physical Chemistry Letters* **15**, 12098 (2024).

[13] A. Mena, S. K. Mann, A. Cowley-Semple, E. Bryan, S. Heutz, D. R. McCamey, M. Attwood, and S. L. Bayliss, Room-temperature optically detected coherent control

of molecular spins, *Physical review letters* **133**, 120801 (2024).

[14] X. Ai, E. W. Evans, S. Dong, A. J. Gillett, H. Guo, Y. Chen, T. J. Hele, R. H. Friend, and F. Li, Efficient radical-based light-emitting diodes with doublet emission, *Nature* **563**, 536 (2018).

[15] R. Chowdhury, P. Murto, N. A. Panjwani, Y. Sun, P. Ghosh, Y. Boeije, C. D. Cordeiro, V. Derkach, S.-J. Woo, O. Millington, *et al.*, Bright triplet and bright charge-separated singlet excitons in organic diradicals enable optical read-out and writing of spin states, *Nature Chemistry* , 1 (2025).

[16] M. Scheidler, U. Lemmer, R. Kersting, S. Karg, W. Riess, B. Cleve, R. Mahrt, H. Kurz, H. Bässler, E. Göbel, *et al.*, Monte carlo study of picosecond exciton relaxation and dissociation in poly (phenylenevinylene), *Physical Review B* **54**, 5536 (1996).

[17] M. M. Yatskou, H. Donker, E. G. Novikov, R. B. Koehorst, A. van Hoek, V. V. Apanasovich, and T. J. Schaaf-sma, Nonisotropic excitation energy transport in organized molecular systems: Monte carlo simulation-based analysis of fluorescence and fluorescence anisotropy decay, *The Journal of Physical Chemistry A* **105**, 9498 (2001).

[18] P. Bobbert, T. Nguyen, F. Van Oost, v. B. Koopmans, and M. Wohlgemant, Bipolaron mechanism for organic magnetoresistance, *Physical review letters* **99**, 216801 (2007).

[19] S. S. Andrews, Using rotational averaging to calculate the bulk response of isotropic and anisotropic samples from molecular parameters, *Journal of chemical education* **81**, 877 (2004).

[20] M. El-Sayed, M. Leung, and C. Lin, Pmdr spectroscopy and the geometry of the triplet state, *Chemical Physics Letters* **14**, 329 (1972).

[21] D. E. Budil and M. C. Thurnauer, The chlorophyll triplet state as a probe of structure and function in photosynthesis, *Biochimica et Biophysica Acta (BBA)-Bioenergetics* **1057**, 1 (1991).

[22] F. Krafft, R. Steyrleuthner, S. Albrecht, D. Neher, M. C. Scharber, R. Bittl, and J. Behrends, Charge separation in pcpdtbt: Pcbm blends from an epr perspective, *The Journal of Physical Chemistry C* **118**, 28482 (2014).

[23] C. W. Beenakker, Random-matrix theory of quantum transport, *Reviews of modern physics* **69**, 731 (1997).

[24] M. L. Mehta, *Random matrices*, Vol. 142 (Elsevier, 2004).

[25] M. Potters and J.-P. Bouchaud, *A first course in random matrix theory: for physicists, engineers and data scientists* (Cambridge University Press, 2020).

[26] Yancita, tiso_deth (2025), GitHub repository.

[27] W. Witschel, Traces of products of angular momentum operators, *Molecular Physics* **22**, 869 (1971).